WIKIPEDIA

Ptychography

Ptychography (/t(ʌ)ɪˈkogræfi/ t(a)i-KO-graf-ee) is a computational method of microscopic imaging.[1] It generates images by processing many coherent interference patterns that have been scattered from an object of interest. Its defining characteristic is translational invariance, which means that the interference patterns are generated by one constant function (e.g. a field of illumination or an aperture stop) moving laterally by a known amount with respect to another constant function (the specimen itself or a wave field). The interference patterns occur some distance away from these two components, so that the scattered waves spread out and "fold" (Ancient Greek: πτύξ is 'fold'[2]) into one another as shown in the figure.

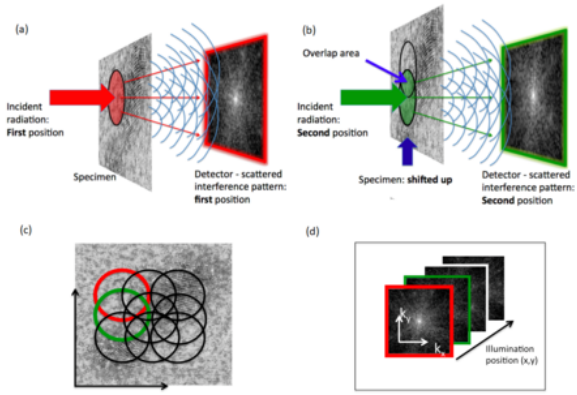

Collection of a ptychographic imaging data set in the simplest single-aperture configuration. (a) Coherent illumination incident from the left is locally confined onto an area of the specimen. A detector downstream of the specimen records an interference pattern. (b) The specimen is shifted (in this case, upwards) and a second pattern is recorded. Note that regions of illumination must overlap with one another to facilitate the ptychographic shift-invariance constraint. (c) A whole ptychographic data set uses many overlapping regions of illumination. (d) The entire data set is four-dimensional: for each 2D illumination position (x, y), there is a 2D diffraction pattern (k_x, k_y).

Ptychography can be used with visible light, X-rays, extreme ultraviolet (EUV) or electrons. Unlike conventional lens imaging, ptychography is unaffected by lens-induced aberrations or diffraction effects caused by limited numerical aperture. This is particularly important for atomic-scale wavelength imaging, where it is difficult and expensive to make good-quality lenses with high numerical aperture. Another important advantage of the technique is that it allows transparent objects to be seen very clearly. This is because it is sensitive to the phase of the radiation that has passed through a specimen,

and so it does not rely on the object absorbing radiation. In the case of visible-light biological microscopy, this means that cells do not need to be stained or labelled to create contrast.

Contents

Phase recovery

Although the interference patterns used in ptychography can only be measured in intensity, the mathematical constraints provided by the translational invariance of the two functions (illumination and object), together with the known shifts between them, means that the phase of the wavefield can be recovered by an inverse computation. Ptychography thus provides a comprehensive solution to the so-called "phase problem". Once this is achieved, all the information relating to the scattered wave (modulus and phase) has been recovered, and so virtually perfect images of the object can be obtained. There are various strategies for performing this inverse phase-retrieval calculation, including direct Wigner distribution deconvolution (WDD)[3] and iterative methods.[4][5][6][7][8] The difference map algorithm developed by Thibault and co-workers[7] is available in a downloadable package called PtyPy (https://ptycho.github.io/ptypy/index.html).[9]

Optical configurations

There are many optical configurations for ptychography: mathematically, it requires two invariant functions that move across one another while an interference pattern generated by the product of the two functions is measured. The interference pattern can be a diffraction pattern, a Fresnel diffraction pattern or, in the case of Fourier ptychography, an image. The "ptycho" convolution in a Fourier ptychographic image derived from the impulse response function of the lens.

The single aperture

This is conceptually the simplest ptychographical arrangement.[10] The detector can either be a long way from the object (i.e. in the Fraunhofer diffraction plane), or closer by, in the Fresnel regime. An advantage of the Fresnel regime is that there is no longer a very high-intensity beam at the centre of the diffraction pattern, which can otherwise saturate the detector pixels there.

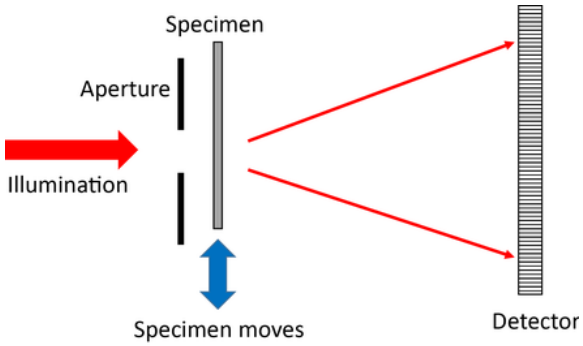

Optical configuration for ptychography using a single aperture

Focused-probe ptychography

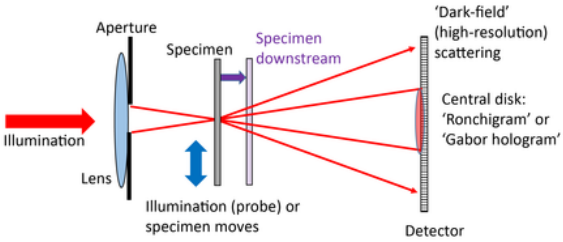

Optical configuration for ptychography using a focused probe

A lens is used to form a tight crossover of the illuminating beam at the plane of the specimen. The configuration is used in the scanning transmission electron microscope (STEM),[11][12] and often in high-resolution X-ray ptychography. The specimen is sometimes shifted up or downstream of the probe crossover so as to allow the size of the patch of illumination to be increased, thus requiring fewer diffraction patterns to scan a wide field of view.

Near-field ptychography

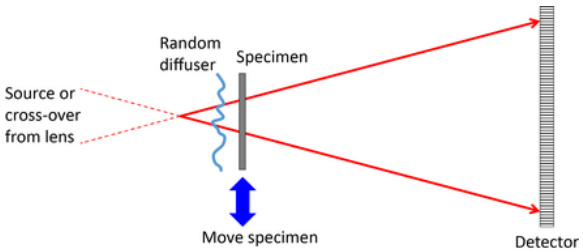

Optical configuration for near-field ptychograhy

This uses a wide field of illumination. To provide magnification, a diverging beam is incident on the specimen. An out-of-focus image, which appears as a Fresnel interference pattern, is projected onto the detector. The illumination must have phase distortions in it, often provided by a diffuser that scrambles the phase of the incident wave before it reaches the specimen, otherwise the image remains constant as the specimen is moved, so there is no new ptychographical information from one position to the next.[13] In the electron microscope, a lens can be used to map the magnified Fresnel image onto the detector.

Fourier ptychography

A conventional microscope is used with a relatively small numerical aperture objective lens. The specimen is illuminated from a series of different angles. Parallel beams coming out of the specimen are brought to a focus in the back focal plane of the objective lens, which is therefore a Fraunhofer diffraction pattern of the specimen exit wave (Abbe's theorem). Tilting the illumination has the effect of shifting the diffraction pattern across the objective aperture (which also lies in the back focal plane). Now the standard ptychographical shift invariance principle applies, except that

the diffraction pattern is acting as the object and the back focal plane stop is acting like the illumination function in conventional ptychography. The image is in the Fraunhofer diffraction plane of these two functions (another consequence of the Abbe's theory), just like in conventional ptychography. The only difference is that the method reconstructs the diffraction pattern, which is much wider than the aperture stop limitation. A final Fourier transform must be undertaken to produce the high-resolution image. All the reconstruction algorithms used in conventional ptychography apply to Fourier ptychography, and indeed nearly all the diverse extensions of conventional ptychography have been used in Fourier ptychography.[14]

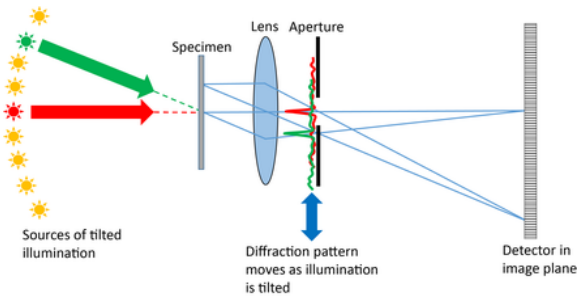

Optical configuration for Fourier ptychography

Imaging ptychography

A lens is used to make a conventional image. An aperture in the image plane acts equivalently to the illumination in conventional ptychography, while the image corresponds to the specimen. The detector lies in the Fraunhofer or Fresnel diffraction plane downstream of the image and aperture.[15]

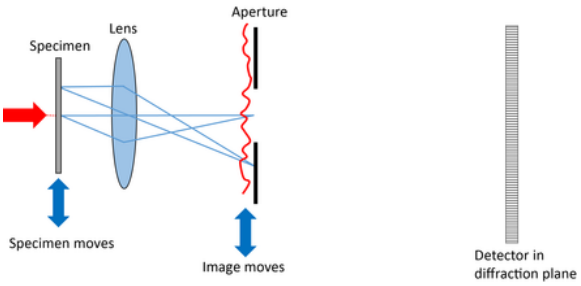

Optical configuration for imaging ptychography

Bragg ptychography or reflection ptychography

This geometry can be used either to map surface features or to measure strain in crystalline specimens. Shifts in the specimen surface, or the atomic Bragg planes perpendicular to the surface, appear in the phase of the ptychographic image.[16][17][18]

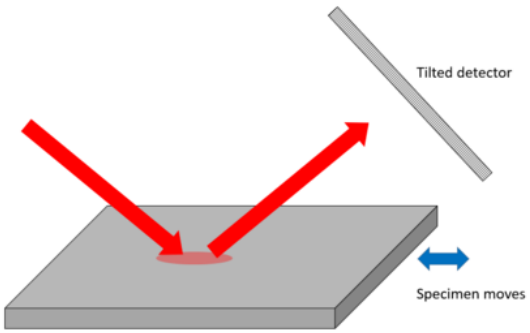

Optical configuration for reflection or Bragg ptychography

Vectorial ptychography

Vectorial ptychography needs to be invoked when the multiplicative model of the interaction between the probe and the specimen cannot be described by scalar quantities.[19] This happens typically when polarized light probes an anisotropic specimen, and when this interaction modifies the state of polarization of light. In that case, the interaction needs to be described by the Jones formalism,[20] where field and object are described by a two-component complex vector and a 2×2 complex matrix respectively. The optical configuration for vectorial ptychography is similar to those of classical (scalar) ptychography, although a control of light polarization (before and after the specimen) needs to be implemented in the setup. Jones maps of the specimens can be retrieved, allowing to quantify a wide range of optical properties (phase, birefringence, orientation of neutral axes, diattenuation, etc.).[21] Similarly to scalar ptychography, the probes used for the measurement can be jointly estimated together with the specimen.[22] As a consequence, vectorial ptychography is also an elegant approach for quantitative imaging of coherent vectorial light beams (mixing wavefront and polarization features).[23]

Advantages

Lens insensitive

Ptychography can be undertaken without using any lenses at all,[10][13] although most implementations use a lens of some type, if only to condense radiation onto the specimen. The detector can measure high angles of scatter, which do not need to pass through a lens. The resolution is therefore only limited by the maximal angle of scatter that reaches the detector, and so avoids the effects of diffraction broadening due to a lens of small numerical aperture or aberrations within the lens. This is key in X-ray, electron and EUV ptychography, where conventional lenses are difficult and expensive to make.

Image phase

Ptychography solves for the phase induced by the real part of the refractive index of the specimen, as well as absorption (the imaginary part of the refractive index). This is crucial for seeing transparent specimens that do not have significant natural absorption contrast, for example biological cells (at visible light wavelengths),[24] thin high-resolution electron

microscopy specimens,[25] and almost all materials at hard X-ray wavelengths. In the latter case, the (linear) phase signal is also ideal for high-resolution X-ray ptychographic tomography.[26] The strength and contrast of the phase signal also means that far fewer photon or electron counts are needed to make an image: this is very important in electron ptychography, where damage to the specimen is a major issue that must be avoided at all costs.[27]

Tolerance to incoherence

Unlike holography, ptychography uses the object itself as an interferometer. It does not require a reference beam. Although holography can solve the image phase problem, it is very difficult to implement in the electron microscope, where the reference beam is extremely sensitive to magnetic interference or other sources of instability. This is why ptychography is not limited by the conventional "information limit" in conventional electron imaging.[28] Furthermore, ptychographical data is sufficiently diverse to remove the effects of partial coherence that would otherwise affect the reconstructed image.[3][29]

Self-calibration

The ptychographical data set can be posed as a blind deconvolution problem.[7][8][30] It has sufficient diversity to solve for both the moving functions (illumination and object), which appear symmetrically in the mathematics of the inversion process. This is now routinely done in any ptychographical experiment, even if the illumination optics have been previously well characterised. Diversity can also be used to solve retrospectively for errors in the offsets of the two functions, blurring in the scan, detector faults, like missing pixels, etc.

Inversion of multiple scattering

In conventional imaging, multiple scattering in a thick sample can seriously complicate, or even entirely invalidate, simple interpretation of an image. This is especially true in electron imaging (where multiple scattering is called "dynamical scattering"). Conversely, ptychography generates

estimates of hundreds or thousands of exit waves, each of which contains different scattering information. This can be used to retrospectively remove multiple scattering effects.[31]

Robustness to noise

The number counts required for a ptychography experiment is the same as for a conventional image, even though the counts are distributed over very many diffraction patterns. This is because dose fractionation applies to ptychography. Maximum-likelihood methods can be employed to reduce the effects of Poisson noise.[32]

Applications

Applications of ptychography are diverse because it can be used with any type of radiation that can be prepared as a quasi-monochromatic propagating wave.

Ptychographic imaging, along with advances in detectors and computing, has resulted in the development of X-ray microscopes.[33][34] Coherent beams are required in order to obtain far-field diffraction patterns with speckle patterns. Coherent X-ray beams can be produced by modern synchrotron radiation sources, free-electron lasers and high-harmonic sources. In terms of routine analysis, X-ray ptychotomography[26] is today the most commonly used technique. It has been applied to many materials problems including, for example, the study of paint,[35] imaging battery chemistry,[36] imaging stacked layers of tandem solar cells,[37] and the dynamics of fracture.[38] In the X-ray regime, ptychography has also been used to obtain a 3D mapping of the disordered structure in the white *Cyphochilus* beetle,[39] and a 2D imaging of the domain structure in a bulk heterojunction for polymer solar cells.[40]

Visible-light ptychography has been used for imaging live biological cells and studying their growth, reproduction and motility.[41] In its vectorial version, it can also be used for mapping quantitative optical properties of anisotropic materials such as biominerals[21] or metasurfaces[42]

Electron ptychography is uniquely (amongst other electron imaging modes) sensitive to both heavy and light atoms simultaneously. It has been used, for example, in the study of nanostructure drug-delivery mechanisms by

looking at drug molecules stained by heavy atoms within light carbon nanotubes cages.[12] With electron beams, shorter-wavelength, higher-energy electrons used for higher-resolution imaging can cause damage to the sample by ionising it and breaking bonds, but electron-beam ptychography has now produced record-breaking images of molybdenum disulphide with a resolution of 0.039 nm using a lower-energy electron beam and detectors that are able to detect single electrons, so atoms can be located with more precision.[27][43]

Ptychography has several applications in the semiconductor industry, including imaging their surfaces using EUV,[44] their 3D bulk structure using X-rays,[45] and mapping strain fields by Bragg ptychography, for example, in nanowires.[46]

Typical ptychographic images

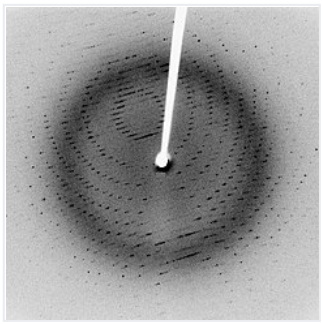

The diffraction pattern of a beam of x-rays passing through a stationary crystal. The dots are areas of constructive interference; the crystal's atomic structure can be worked out from the pattern. In ptychography, a sample (which does not need to be crystalline) is moved sequentially through the beam, creating a range of diffraction patterns.

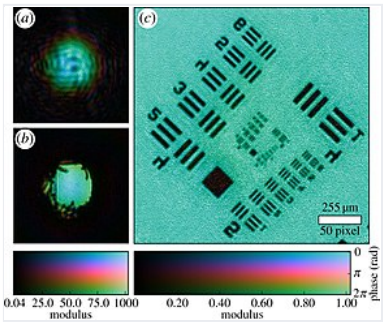

A visible-light ptychograph of a USAF optical resolution target, made using a pinhole aperture in a piece of cardboard. In the graphs, the hue represents the phase, and the modulus represents the luminance. (a) shows a single image with complex diffraction detail. (b) shows the computer-processed version of (a). (c) shows the result from combined computer-processed diffraction data after the whole sample was scanned.[47]

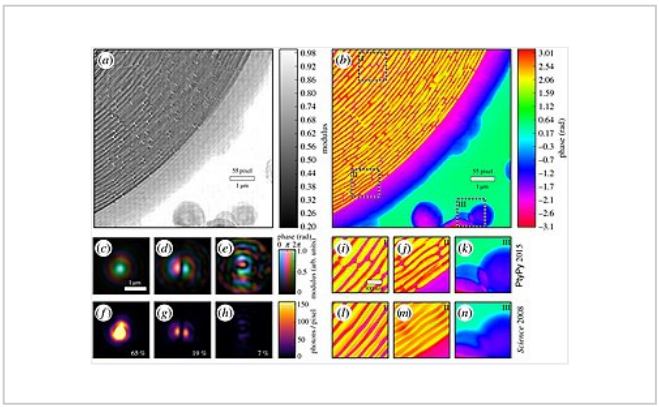

X-ray ptychography at a small-angle scattering beamline of a synchrotron. This x-ray ptychograph of a zone plate shows the luminosity data in image (a) and the phase data in image (b). Insets I, II and III from (b) are shown in (i), (j) and (k) respectively as processed in 2015; they show a clear improvement in resolution over the algorithms used in 2008 shown in (l), (m) and (n).

History

Beginnings in crystallography

The name "ptychography" was coined by Hegerl and Hoppe in 1970[48] to describe a solution to the crystallographic phase problem first suggested by Hoppe in 1969.[49] The idea required the specimen to be highly ordered (a crystal) and to be illuminated by a precisely engineered wave so that only two pairs of diffraction peaks interfere with one another at a time. A shift in the illumination changes the interference condition (by the Fourier shift theorem). The two measurements can be used to solve for the relative phase between the two diffraction peaks by breaking a complex-conjugate ambiguity that would otherwise exist.[50] Although the idea encapsulates the underlying concept of interference by convolution (ptycho) and translational invariance, crystalline ptychography cannot be used for

imaging of continuous objects, because very many (up to millions) of beams interfere at the same time, and so the phase differences are inseparable. Hoppe abandoned his concept of ptychography in 1973.

Development of inversion methods

Between 1989 and 2007 Rodenburg and co-workers developed various inversion methods for the general imaging ptychographic phase problem, including Wigner-distribution deconvolution (WDD),[3] SSB,[11] the "PIE" iterative method[4] (a precursor of the "ePIE" algorithm[8]), demonstrating proof-of-principles at various wavelengths.[11][51][52] Chapman used the WDD inversion method to demonstrate the first implementation of X-ray ptychography in 1996.[53] The smallness of computers and poor quality of detectors at that time may account for the fact that ptychography was not at first taken up by other workers.

General uptake

Widespread interest in ptychography only started after the first demonstration of iterative phase-retrieval X-ray ptychography in 2007 at the Swiss Light Source (SLS).[52] Progress at X-ray wavelengths was then quick. By 2010, the SLS had developed X-ray ptychotomography,[26] now a major application of the technique. Thibault, also working at the SLS, developed the difference-map (DM) iterative inversion algorithm and mixed-state ptychography.[7][29] Since 2010, several groups have developed the capabilities of ptychography to characterize and improve reflective[54] and refractive X-ray optics.[55][56] Bragg ptychography, for measuring strain in crystals, was demonstrated by Hruszkewycz in 2012.[16] In 2012 it was also shown that electron ptychography could improve on the resolution of an electron lens by a factor of five,[57] a method which was used in 2018 to provide the highest-resolution transmission image ever obtained[27] earning a Guinness world record,[58] and once again in 2021 to achieve an even better resolution.[59][60][61] Real-space light ptychography became available in a commercial system (https://www.phasefocus.com/) for live-cell imaging in 2013.[24] Fourier ptychography using iterative methods was also demonstrated by Zheng et al.[14] in 2013, a field which is growing rapidly. The group of Margaret Murnane and Henry Kapteyn at JILA, CU Boulder demonstrated EUV reflection ptychographic imaging in 2014.[17]

See also

- Phase retrieval
- Computational imaging
- Fourier ptychography

References

1. Rodenburg J, Maiden A (2019). "Ptychography". In Hawkes PW, Spence JC (eds.). *Springer Handbook of Microscopy* (https://eprints.whiterose.ac.uk/127795/1/Ptychography_Chapter-Rodenburg%2BMaiden_final.pdf) (PDF). Springer Handbooks. Springer International Publishing. pp. 819–904. doi:10.1007/978-3-030-00069-1_17 (https://doi.org/10.1007%2F978-3-030-00069-1_17). ISBN 978-3-030-00068-4.
2. Hegerl R, Hoppe W (1970). "Dynamische Theorie der Kristallstrukturanalyse durch Elektronenbeugung im inhomogenen Primärstrahlwellenfeld". *Berichte der Bunsengesellschaft für physikalische Chemie* (in German). **74** (11): 1148–1154. doi:10.1002/bbpc.19700741112 (https://doi.org/10.1002%2Fbbpc.19700741112).
3. Rodenburg J, Bates RH (15 June 1992). "The theory of super-resolution electron microscopy via Wigner-distribution deconvolution". *Phil. Trans. R. Soc. Lond. A*. **339** (1655): 521–553. Bibcode:1992RSPTA.339..521R (https://ui.adsabs.harvard.edu/abs/1992RSPTA.339..521R). doi:10.1098/rsta.1992.0050 (https://doi.org/10.1098%2Frsta.1992.0050). S2CID 123384269 (https://api.semanticscholar.org/CorpusID:123384269).
4. Rodenburg JM, Faulkner HM (15 November 2004). "A phase retrieval algorithm for shifting illumination". *Applied Physics Letters*. **85** (20): 4795–4797. Bibcode:2004ApPhL..85.4795R (https://ui.adsabs.harvard.edu/abs/2004ApPhL..85.4795R). doi:10.1063/1.1823034 (https://doi.org/10.1063%2F1.1823034).
5. Guizar-Sicairos M, Fienup JR (May 2008). "Phase retrieval with transverse translation diversity: a nonlinear optimization approach" (https://doi.org/10.1364%2FOE.16.007264). *Optics Express*. **16** (10): 7264–78. Bibcode:2008OExpr..16.7264G (https://ui.adsabs.harvard.edu/abs/2008OExpr..16.7264G). doi:10.1364/OE.16.007264 (https://doi.org/10.1364%2FOE.16.007264). PMID 18545432 (https://pubmed.ncbi.nlm.nih.gov/18545432).

6. Thibault P, Dierolf M, Menzel A, Bunk O, David C, Pfeiffer F (July 2008). "High-resolution scanning x-ray diffraction microscopy". *Science*. **321** (5887): 379–82. Bibcode:2008Sci...321..379T (https://ui.adsabs.harvard.edu/abs/2008Sci...321..379T). doi:10.1126/science.1158573 (https://doi.org/10.1126%2Fscience.1158573). PMID 18635796 (https://pubmed.ncbi.nlm.nih.gov/18635796). S2CID 30125688 (https://api.semanticscholar.org/CorpusID:30125688).
7. Thibault P, Dierolf M, Bunk O, Menzel A, Pfeiffer F (March 2009). "Probe retrieval in ptychographic coherent diffractive imaging". *Ultramicroscopy*. **109** (4): 338–43. doi:10.1016/j.ultramic.2008.12.011 (https://doi.org/10.1016%2Fj.ultramic.2008.12.011). PMID 19201540 (https://pubmed.ncbi.nlm.nih.gov/19201540).
8. Maiden AM, Rodenburg JM (September 2009). "An improved ptychographical phase retrieval algorithm for diffractive imaging". *Ultramicroscopy*. **109** (10): 1256–62. doi:10.1016/j.ultramic.2009.05.012 (https://doi.org/10.1016%2Fj.ultramic.2009.05.012). PMID 19541420 (https://pubmed.ncbi.nlm.nih.gov/19541420).
9. Enders B, Thibault P (December 2016). "A computational framework for ptychographic reconstructions" (https://www.ncbi.nlm.nih.gov/pmc/articles/PMC5247528). *Proceedings of the Royal Society A: Mathematical, Physical and Engineering Sciences*. **472** (2196): 20160640. Bibcode:2016RSPSA.47260640E (https://ui.adsabs.harvard.edu/abs/2016RSPSA.47260640E). doi:10.1098/rspa.2016.0640 (https://doi.org/10.1098%2Frspa.2016.0640). PMC 5247528 (https://www.ncbi.nlm.nih.gov/pmc/articles/PMC5247528). PMID 28119552 (https://pubmed.ncbi.nlm.nih.gov/28119552).
10. Rodenburg JM, Hurst AC, Cullis AG (February 2007). "Transmission microscopy without lenses for objects of unlimited size". *Ultramicroscopy*. **107** (2–3): 227–231. doi:10.1016/j.ultramic.2006.07.007 (https://doi.org/10.1016%2Fj.ultramic.2006.07.007). PMID 16959428 (https://pubmed.ncbi.nlm.nih.gov/16959428).
11. Rodenburg JM, McCallum BC, Nellist PD (March 1993). "Experimental tests on double-resolution coherent imaging via STEM". *Ultramicroscopy*. **48** (3): 304–314. doi:10.1016/0304-3991(93)90105-7 (https://doi.org/10.1016%2F0304-3991%2893%2990105-7). ISSN 0304-3991 (https://www.worldcat.org/issn/0304-3991).

12. Yang H, Rutte RN, Jones L, Simson M, Sagawa R, Ryll H, et al. (August 2016). "Simultaneous atomic-resolution electron ptychography and Z-contrast imaging of light and heavy elements in complex nanostructures" (https://www.ncbi.nlm.nih.gov/pmc/articles/PMC5007440). *Nature Communications*. **7**: 12532. Bibcode:2016NatCo...712532Y (https://ui.adsabs.harvard.edu/abs/2016NatCo...712532Y). doi:10.1038/ncomms12532 (https://doi.org/10.1038%2Fncomms12532). PMC 5007440 (https://www.ncbi.nlm.nih.gov/pmc/articles/PMC5007440). PMID 27561914 (https://pubmed.ncbi.nlm.nih.gov/27561914).
13. Stockmar M, Cloetens P, Zanette I, Enders B, Dierolf M, Pfeiffer F, Thibault P (31 May 2013). "Near-field ptychography: phase retrieval for inline holography using a structured illumination" (https://www.ncbi.nlm.nih.gov/pmc/articles/PMC3668322). *Scientific Reports*. **3** (1): 1927. Bibcode:2013NatSR...3E1927S (https://ui.adsabs.harvard.edu/abs/2013NatSR...3E1927S). doi:10.1038/srep01927 (https://doi.org/10.1038%2Fsrep01927). PMC 3668322 (https://www.ncbi.nlm.nih.gov/pmc/articles/PMC3668322). PMID 23722622 (https://pubmed.ncbi.nlm.nih.gov/23722622).
14. Zheng G, Horstmeyer R, Yang C (September 2013). "Wide-field, high-resolution Fourier ptychographic microscopy" (https://www.ncbi.nlm.nih.gov/pmc/articles/PMC4169052). *Nature Photonics*. **7** (9): 739–745. arXiv:1405.0226 (https://arxiv.org/abs/1405.0226). Bibcode:2013NaPho...7..739Z (https://ui.adsabs.harvard.edu/abs/2013NaPho...7..739Z). doi:10.1038/nphoton.2013.187 (https://doi.org/10.1038%2Fnphoton.2013.187). PMC 4169052 (https://www.ncbi.nlm.nih.gov/pmc/articles/PMC4169052). PMID 25243016 (https://pubmed.ncbi.nlm.nih.gov/25243016).
15. Maiden AM, Sarahan MC, Stagg MD, Schramm SM, Humphry MJ (October 2015). "Quantitative electron phase imaging with high sensitivity and an unlimited field of view" (https://www.ncbi.nlm.nih.gov/pmc/articles/PMC4589788). *Scientific Reports*. **5**: 14690. Bibcode:2015NatSR...514690M (https://ui.adsabs.harvard.edu/abs/2015NatSR...514690M). doi:10.1038/srep14690 (https://doi.org/10.1038%2Fsrep14690). PMC 4589788 (https://www.ncbi.nlm.nih.gov/pmc/articles/PMC4589788). PMID 26423558 (https://pubmed.ncbi.nlm.nih.gov/26423558).

16. Hruszkewycz SO, Holt MV, Murray CE, Bruley J, Holt J, Tripathi A, et al. (October 2012). "Quantitative nanoscale imaging of lattice distortions in epitaxial semiconductor heterostructures using nanofocused X-ray Bragg projection ptychography". *Nano Letters*. **12** (10): 5148–5154. Bibcode:2012NanoL..12.5148H (https://ui.adsabs.harvard.edu/abs/2012NanoL..12.5148H). doi:10.1021/nl303201w (https://doi.org/10.1021%2Fnl303201w). PMID 22998744 (https://pubmed.ncbi.nlm.nih.gov/22998744).
17. Seaberg MD, Zhang B, Gardner DF, Shanblatt ER, Murnane MM, Kapteyn HC, Adams DE (22 July 2014). "Tabletop nanometer extreme ultraviolet imaging in an extended reflection mode using coherent Fresnel ptychography". *Optica*. **1** (1): 39–44. arXiv:1312.2049 (https://arxiv.org/abs/1312.2049). Bibcode:2014Optic...1...39S (https://ui.adsabs.harvard.edu/abs/2014Optic...1...39S). doi:10.1364/OPTICA.1.000039 (https://doi.org/10.1364%2FOPTICA.1.000039). ISSN 2334-2536 (https://www.worldcat.org/issn/2334-2536). S2CID 10577107 (https://api.semanticscholar.org/CorpusID:10577107).
18. Godard, P.; Carbone, G.; Allain, M.; Mastropietro, F.; Chen, G.; Capello, L.; Diaz, A.; Metzger, T.H.; Stangl, J.; Chamard, V. (2011). "Three-dimensional high-resolution quantitative microscopy of extended crystals" (http://www.nature.com/articles/ncomms1569). *Nature Communications*. **2** (1): 568. doi:10.1038/ncomms1569 (https://doi.org/10.1038%2Fncomms1569). ISSN 2041-1723 (https://www.worldcat.org/issn/2041-1723). PMID 22127064 (https://pubmed.ncbi.nlm.nih.gov/22127064).
19. Ferrand P, Allain M, Chamard V (November 2015). "Ptychography in anisotropic media" (https://hal.archives-ouvertes.fr/hal-01213942/file/Ferrand-OL-2015.pdf) (PDF). *Optics Letters*. **40** (22): 5144–5147. Bibcode:2015OptL...40.5144F (https://ui.adsabs.harvard.edu/abs/2015OptL...40.5144F). doi:10.1364/OL.40.005144 (https://doi.org/10.1364%2FOL.40.005144). PMID 26565820 (https://pubmed.ncbi.nlm.nih.gov/26565820).
20. Jones RC (1 July 1941). "A New Calculus for the Treatment of Optical SystemsI. Description and Discussion of the Calculus". *JOSA*. **31** (7): 488–493. doi:10.1364/JOSA.31.000488 (https://doi.org/10.1364%2FJOSA.31.000488).

21. Ferrand P, Baroni A, Allain M, Chamard V (February 2018). "Quantitative imaging of anisotropic material properties with vectorial ptychography". *Optics Letters*. **43** (4): 763–766. arXiv:1712.00260 (https://arxiv.org/abs/1712.00260). Bibcode:2018OptL...43..763F (https://ui.adsabs.harvard.edu/abs/2018OptL...43..763F). doi:10.1364/OL.43.000763 (https://doi.org/10.1364%2FOL.43.000763). PMID 29443988 (https://pubmed.ncbi.nlm.nih.gov/29443988). S2CID 3433117 (https://api.semanticscholar.org/CorpusID:3433117).
22. Baroni A, Allain M, Li P, Chamard V, Ferrand P (March 2019). "Joint estimation of object and probes in vectorial ptychography" (https://hal-amu.archives-ouvertes.fr/hal-02059897/file/Baroni-oe-27-6-8143.pdf) (PDF). *Optics Express*. **27** (6): 8143–8152. Bibcode:2019OExpr..27.8143B (https://ui.adsabs.harvard.edu/abs/2019OExpr..27.8143B). doi:10.1364/OE.27.008143 (https://doi.org/10.1364%2FOE.27.008143). PMID 31052637 (https://pubmed.ncbi.nlm.nih.gov/31052637).
23. Baroni A, Ferrand P (November 2020). "Reference-free quantitative microscopic imaging of coherent arbitrary vectorial light beams" (https://www.osapublishing.org/abstract.cfm?URI=oe-28-23-35339). *Optics Express*. **28** (23): 35339–35349. Bibcode:2020OExpr..2835339B (https://ui.adsabs.harvard.edu/abs/2020OExpr..2835339B). doi:10.1364/OE.408665 (https://doi.org/10.1364%2FOE.408665). PMID 33182982 (https://pubmed.ncbi.nlm.nih.gov/33182982).
24. Marrison J, Räty L, Marriott P, O'Toole P (6 August 2013). "Ptychography--a label free, high-contrast imaging technique for live cells using quantitative phase information" (https://www.ncbi.nlm.nih.gov/pmc/articles/PMC3734479). *Scientific Reports*. **3** (1): 2369. Bibcode:2013NatSR...3E2369M (https://ui.adsabs.harvard.edu/abs/2013NatSR...3E2369M). doi:10.1038/srep02369 (https://doi.org/10.1038%2Fsrep02369). PMC 3734479 (https://www.ncbi.nlm.nih.gov/pmc/articles/PMC3734479). PMID 23917865 (https://pubmed.ncbi.nlm.nih.gov/23917865).
25. Yang H, MacLaren I, Jones L, Martinez GT, Simson M, Huth M, et al. (September 2017). "Electron ptychographic phase imaging of light elements in crystalline materials using Wigner distribution deconvolution" (https://doi.org/10.1016%2Fj.ultramic.2017.02.006). *Ultramicroscopy*. **180**: 173–179. doi:10.1016/j.ultramic.2017.02.006 (https://doi.org/10.1016%2Fj.ultramic.2017.02.006). PMID 28434783 (https://pubmed.ncbi.nlm.nih.gov/28434783).

26. Dierolf M, Menzel A, Thibault P, Schneider P, Kewish CM, Wepf R, et al. (September 2010). "Ptychographic X-ray computed tomography at the nanoscale". *Nature*. **467** (7314): 436–439. Bibcode:2010Natur.467..436D (https://ui.adsabs.harvard.edu/abs/2010Natur.467..436D). doi:10.1038/nature09419 (https://doi.org/10.1038%2Fnature09419). PMID 20864997 (https://pubmed.ncbi.nlm.nih.gov/20864997). S2CID 2449015 (https://api.semanticscholar.org/CorpusID:2449015).
27. Jiang Y, Chen Z, Han Y, Deb P, Gao H, Xie S, et al. (July 2018). "Electron ptychography of 2D materials to deep sub-ångström resolution". *Nature*. **559** (7714): 343–349. Bibcode:2018Natur.559..343J (https://ui.adsabs.harvard.edu/abs/2018Natur.559..343J). doi:10.1038/s41586-018-0298-5 (https://doi.org/10.1038%2Fs41586-018-0298-5). PMID 30022131 (https://pubmed.ncbi.nlm.nih.gov/30022131). S2CID 49865457 (https://api.semanticscholar.org/CorpusID:49865457).
28. Nellist P, McCallum B, Rodenburg JM (April 1995). "Resolution beyond the 'information limit' in transmission electron microscopy". *Nature*. **374** (6523): 630–632. Bibcode:1995Natur.374..630N (https://ui.adsabs.harvard.edu/abs/1995Natur.374..630N). doi:10.1038/374630a0 (https://doi.org/10.1038%2F374630a0). S2CID 4330017 (https://api.semanticscholar.org/CorpusID:4330017).
29. Thibault P, Menzel A (February 2013). "Reconstructing state mixtures from diffraction measurements". *Nature*. **494** (7435): 68–71. Bibcode:2013Natur.494...68T (https://ui.adsabs.harvard.edu/abs/2013Natur.494...68T). doi:10.1038/nature11806 (https://doi.org/10.1038%2Fnature11806). PMID 23389541 (https://pubmed.ncbi.nlm.nih.gov/23389541). S2CID 4424305 (https://api.semanticscholar.org/CorpusID:4424305).
30. McCallum BC, Rodenburg JM (1 February 1993). "Simultaneous reconstruction of object and aperture functions from multiple far-field intensity measurements". *JOSA A*. **10** (2): 231–239. Bibcode:1993JOSAA..10..231M (https://ui.adsabs.harvard.edu/abs/1993JOSAA..10..231M). doi:10.1364/JOSAA.10.000231 (https://doi.org/10.1364%2FJOSAA.10.000231).

31. Maiden AM, Humphry MJ, Rodenburg JM (August 2012). "Ptychographic transmission microscopy in three dimensions using a multi-slice approach". *Journal of the Optical Society of America A*. **29** (8): 1606–1614. Bibcode:2012JOSAA..29.1606M (https://ui.adsabs.harvard.edu/abs/2012JOSAA..29.1606M). doi:10.1364/JOSAA.29.001606 (https://doi.org/10.1364%2FJOSAA.29.001606). PMID 23201876 (https://pubmed.ncbi.nlm.nih.gov/23201876).
32. Thibault P, Guizar-Sicairos M (2012). "Maximum-likelihood refinement for coherent diffractive imaging" (https://doi.org/10.1088%2F1367-2630%2F14%2F6%2F063004). *New Journal of Physics*. **14** (6): 063004. Bibcode:2012NJPh...14f3004T (https://ui.adsabs.harvard.edu/abs/2012NJPh...14f3004T). doi:10.1088/1367-2630/14/6/063004 (https://doi.org/10.1088%2F1367-2630%2F14%2F6%2F063004).
33. Chapman HN (September 2010). "Microscopy: A new phase for X-ray imaging". *Nature*. **467** (7314): 409–410. Bibcode:2010Natur.467..409C (https://ui.adsabs.harvard.edu/abs/2010Natur.467..409C). doi:10.1038/467409a (https://doi.org/10.1038%2F467409a). PMID 20864990 (https://pubmed.ncbi.nlm.nih.gov/20864990). S2CID 205058970 (https://api.semanticscholar.org/CorpusID:205058970).
34. "Ptychography" (https://www-ssrl.slac.stanford.edu/wekergroup/ptychography). *www6.slac.stanford.edu*. Retrieved 29 July 2018.
35. Chen B, Guizar-Sicairos M, Xiong G, Shemilt L, Diaz A, Nutter J, et al. (31 January 2013). "Three-dimensional structure analysis and percolation properties of a barrier marine coating" (https://www.ncbi.nlm.nih.gov/pmc/articles/PMC3558722). *Scientific Reports*. **3** (1): 1177. Bibcode:2013NatSR...3E1177C (https://ui.adsabs.harvard.edu/abs/2013NatSR...3E1177C). doi:10.1038/srep01177 (https://doi.org/10.1038%2Fsrep01177). PMC 3558722 (https://www.ncbi.nlm.nih.gov/pmc/articles/PMC3558722). PMID 23378910 (https://pubmed.ncbi.nlm.nih.gov/23378910).
36. Shapiro DA, Yu YS, Tyliszczak T, Cabana J, Celestre R, Chao W, et al. (7 September 2014). "Chemical composition mapping with nanometre resolution by soft X-ray microscopy". *Nature Photonics*. **8** (10): 765–769. Bibcode:2014NaPho...8..765S (https://ui.adsabs.harvard.edu/abs/2014NaPho...8..765S). doi:10.1038/nphoton.2014.207 (https://doi.org/10.1038%2Fnphoton.2014.207). ISSN 1749-4885 (https://www.worldcat.org/issn/1749-4885).

37. Pedersen EB, Angmo D, Dam HF, Thydén KT, Andersen TR, Skjønsfjell ET, et al. (August 2015). "Improving organic tandem solar cells based on water-processed nanoparticles by quantitative 3D nanoimaging". *Nanoscale*. **7** (32): 13765–13774. Bibcode:2015Nanos...713765P (https://ui.adsabs.harvard.edu/abs/2015Nanos...713765P). doi:10.1039/C5NR02824H (https://doi.org/10.1039%2FC5NR02824H). PMID 26220159 (https://pubmed.ncbi.nlm.nih.gov/26220159).
38. Bo Flyostad J, Skjnsfjell ET, GuizarSicairos M, Hydalsvik K, He J, Andreasen JW, et al. (10 February 2015). "Quantitative 3D X-ray Imaging of Densification, Delamination and Fracture in a Micro-Composite under Compression" (https://backend.orbit.dtu.dk/ws/files/119895493/Quantitative_3D_X_ray_Imaging_of_Densification_postprint.pdf) (PDF). *Advanced Engineering Materials* (Submitted manuscript). **17** (4): 545–553. doi:10.1002/adem.201400443 (https://doi.org/10.1002%2Fadem.201400443). ISSN 1438-1656 (https://www.worldcat.org/issn/1438-1656).
39. Wilts BD, Sheng X, Holler M, Diaz A, Guizar-Sicairos M, Raabe J, et al. (May 2018). "Evolutionary-Optimized Photonic Network Structure in White Beetle Wing Scales" (https://doi.org/10.1002%2Fadma.201702057). *Advanced Materials*. **30** (19): e1702057. doi:10.1002/adma.201702057 (https://doi.org/10.1002%2Fadma.201702057). PMID 28640543 (https://pubmed.ncbi.nlm.nih.gov/28640543).
40. Patil N, Skjønsfjell ET, Van den Brande N, Chavez Panduro EA, Claessens R, Guizar-Sicairos M, et al. (July 2016). "X-Ray Nanoscopy of a Bulk Heterojunction" (https://www.ncbi.nlm.nih.gov/pmc/articles/PMC4930208). *PLOS ONE*. **11** (7): e0158345. Bibcode:2016PLoSO..1158345P (https://ui.adsabs.harvard.edu/abs/2016PLoSO..1158345P). doi:10.1371/journal.pone.0158345 (https://doi.org/10.1371%2Fjournal.pone.0158345). PMC 4930208 (https://www.ncbi.nlm.nih.gov/pmc/articles/PMC4930208). PMID 27367796 (https://pubmed.ncbi.nlm.nih.gov/27367796).
41. Kasprowicz R, Suman R, O'Toole P (March 2017). "Characterising live cell behaviour: Traditional label-free and quantitative phase imaging approaches" (https://doi.org/10.1016%2Fj.biocel.2017.01.004). *The International Journal of Biochemistry & Cell Biology*. **84**: 89–95. doi:10.1016/j.biocel.2017.01.004 (https://doi.org/10.1016%2Fj.biocel.2017.01.004). PMID 28111333 (https://pubmed.ncbi.nlm.nih.gov/28111333).

42. Song Q, Baroni A, Sawant R, Ni P, Brandli V, Chenot S, et al. (May 2020). "Ptychography retrieval of fully polarized holograms from geometric-phase metasurfaces" (https://www.ncbi.nlm.nih.gov/pmc/articles/PMC7253437). *Nature Communications*. **11** (1): 2651. Bibcode:2020NatCo..11.2651S (https://ui.adsabs.harvard.edu/abs/2020NatCo..11.2651S). doi:10.1038/s41467-020-16437-9 (https://doi.org/10.1038%2Fs41467-020-16437-9). PMC 7253437 (https://www.ncbi.nlm.nih.gov/pmc/articles/PMC7253437). PMID 32461637 (https://pubmed.ncbi.nlm.nih.gov/32461637).
43. Wogan T (26 July 2018). "Electron images achieve record-breaking resolution" (https://physicsworld.com/a/electron-images-achieve-record-breaking-resolution/). *Physics World*. **31** (9): 5. Bibcode:2018PhyW...31i...5W (https://ui.adsabs.harvard.edu/abs/2018PhyW...31i...5W). doi:10.1088/2058-7058/31/9/8 (https://doi.org/10.1088%2F2058-7058%2F31%2F9%2F8). Retrieved 27 July 2018.
44. Zhang B, Gardner DF, Seaberg MD, Shanblatt ER, Kapteyn HC, Murnane MM, Adams DE (November 2015). "High contrast 3D imaging of surfaces near the wavelength limit using tabletop EUV ptychography" (https://doi.org/10.1016%2Fj.ultramic.2015.07.006). *Ultramicroscopy*. **158**: 98–104. doi:10.1016/j.ultramic.2015.07.006 (https://doi.org/10.1016%2Fj.ultramic.2015.07.006). PMID 26233823 (https://pubmed.ncbi.nlm.nih.gov/26233823).
45. Holler M, Guizar-Sicairos M, Tsai EH, Dinapoli R, Müller E, Bunk O, et al. (March 2017). "High-resolution non-destructive three-dimensional imaging of integrated circuits". *Nature*. **543** (7645): 402–406. Bibcode:2017Natur.543..402H (https://ui.adsabs.harvard.edu/abs/2017Natur.543..402H). doi:10.1038/nature21698 (https://doi.org/10.1038%2Fnature21698). PMID 28300088 (https://pubmed.ncbi.nlm.nih.gov/28300088). S2CID 4448836 (https://api.semanticscholar.org/CorpusID:4448836).
46. Hill MO, Calvo-Almazan I, Allain M, Holt MV, Ulvestad A, Treu J, et al. (February 2018). "Measuring Three-Dimensional Strain and Structural Defects in a Single InGaAs Nanowire Using Coherent X-ray Multiangle Bragg Projection Ptychography" (https://hal.archives-ouvertes.fr/hal-01687989/file/Hill_maBPP_final.pdf) (PDF). *Nano Letters*. **18** (2): 811–819. Bibcode:2018NanoL..18..811H (https://ui.adsabs.harvard.edu/abs/2018NanoL..18..811H). doi:10.1021/acs.nanolett.7b04024 (https://doi.org/10.1021%2Facs.nanolett.7b04024). PMID 29345956 (https://pubmed.ncbi.nlm.nih.gov/29345956).

47. Enders B, Thibault P (December 2016). "A computational framework for ptychographic reconstructions" (https://www.ncbi.nlm.nih.gov/pmc/articles/PMC5247528). *Proceedings of the Royal Society A: Mathematical, Physical and Engineering Sciences*. **472** (2196): 20160640. Bibcode:2016RSPSA.47260640E (https://ui.adsabs.harvard.edu/abs/2016RSPSA.47260640E). doi:10.1098/rspa.2016.0640 (https://doi.org/10.1098%2Frspa.2016.0640). PMC 5247528 (https://www.ncbi.nlm.nih.gov/pmc/articles/PMC5247528). PMID 28119552 (https://pubmed.ncbi.nlm.nih.gov/28119552).
48. Hegerl R, Hoppe W (November 1970). "Dynamische Theorie der Kristallstrukturanalyse durch Elektronenbeugung im inhomogenen Primärstrahlwellenfeld". *Berichte der Bunsengesellschaft für Physikalische Chemie* (in German). **74** (11): 1148–1154. doi:10.1002/bbpc.19700741112 (https://doi.org/10.1002%2Fbbpc.19700741112). ISSN 0005-9021 (https://www.worldcat.org/issn/0005-9021).
49. Hoppe W (1969). "Beugung im inhomogenen Primärstrahlwellenfeld. I. Prinzip einer Phasenmessung von Elektronenbeugungsinterferenzen". *Acta Crystallographica Section A* (in German). **25** (4): 495–501. Bibcode:1969AcCrA..25..495H (https://ui.adsabs.harvard.edu/abs/1969AcCrA..25..495H). doi:10.1107/S0567739469001045 (https://doi.org/10.1107%2FS0567739469001045).
50. Rodenburg JM (2008). "Ptychography and Related Diffractive Imaging Methods". *Advances in Imaging and Electron Physics*. Advances in Imaging and Electron Physics. Vol. 150. Elsevier. pp. 87–184. doi:10.1016/s1076-5670(07)00003-1 (https://doi.org/10.1016%2Fs1076-5670%2807%2900003-1). ISBN 9780123742179.
51. Friedman SL, Rodenburg JM (1992). "Optical demonstration of a new principle of far-field microscopy". *Journal of Physics D: Applied Physics*. **25** (2): 147–154. Bibcode:1992JPhD...25..147F (https://ui.adsabs.harvard.edu/abs/1992JPhD...25..147F). doi:10.1088/0022-3727/25/2/003 (https://doi.org/10.1088%2F0022-3727%2F25%2F2%2F003). ISSN 0022-3727 (https://www.worldcat.org/issn/0022-3727).
52. Rodenburg JM, Hurst AC, Cullis AG, Dobson BR, Pfeiffer F, Bunk O, et al. (January 2007). "Hard-x-ray lensless imaging of extended objects" (https://www.dora.lib4ri.ch/psi/islandora/object/psi%3A18137). *Physical Review Letters*. **98** (3): 034801. Bibcode:2007PhRvL..98c4801R (https://ui.adsabs.harvard.edu/abs/2007PhRvL..98c4801R). doi:10.1103/PhysRevLett.98.034801 (https://doi.org/10.1103%2FPhysRevLett.98.034801). PMID 17358687 (https://pubmed.ncbi.nlm.nih.gov/17358687).

53. Chapman HN (December 1996). "Phase-retrieval X-ray microscopy by Wigner-distribution deconvolution". *Ultramicroscopy*. **66** (3–4): 153–172. doi:10.1016/s0304-3991(96)00084-8 (https://doi.org/10.1016%2Fs0304-3991%2896%2900084-8). ISSN 0304-3991 (https://www.worldcat.org/issn/0304-3991).
54. Kewish CM, Thibault P, Dierolf M, Bunk O, Menzel A, Vila-Comamala J, et al. (March 2010). "Ptychographic characterization of the wavefield in the focus of reflective hard X-ray optics". *Ultramicroscopy*. **110** (4): 325–329. doi:10.1016/j.ultramic.2010.01.004 (https://doi.org/10.1016%2Fj.ultramic.2010.01.004). PMID 20116927 (https://pubmed.ncbi.nlm.nih.gov/20116927).
55. Schropp A, Boye P, Feldkamp JM, Hoppe R, Patommel J, Samberg D, et al. (March 2010). "Hard x-ray nanobeam characterization by coherent diffraction microscopy". *Applied Physics Letters*. **96** (9): 091102. Bibcode:2010ApPhL..96i1102S (https://ui.adsabs.harvard.edu/abs/2010ApPhL..96i1102S). doi:10.1063/1.3332591 (https://doi.org/10.1063%2F1.3332591). ISSN 0003-6951 (https://www.worldcat.org/issn/0003-6951).
56. Guizar-Sicairos M, Narayanan S, Stein A, Metzler M, Sandy AR, Fienup JR, Evans-Lutterodt K (March 2011). "Measurement of hard x-ray lens wavefront aberrations using phase retrieval" (https://www.dora.lib4ri.ch/psi/islandora/object/psi%3A14057). *Applied Physics Letters*. **98** (11): 111108. Bibcode:2011ApPhL..98k1108G (https://ui.adsabs.harvard.edu/abs/2011ApPhL..98k1108G). doi:10.1063/1.3558914 (https://doi.org/10.1063%2F1.3558914). ISSN 0003-6951 (https://www.worldcat.org/issn/0003-6951).
57. Humphry MJ, Kraus B, Hurst AC, Maiden AM, Rodenburg JM (March 2012). "Ptychographic electron microscopy using high-angle dark-field scattering for sub-nanometre resolution imaging" (https://www.ncbi.nlm.nih.gov/pmc/articles/PMC3316878). *Nature Communications*. **3** (370): 730. Bibcode:2012NatCo...3..730H (https://ui.adsabs.harvard.edu/abs/2012NatCo...3..730H). doi:10.1038/ncomms1733 (https://doi.org/10.1038%2Fncomms1733). PMC 3316878 (https://www.ncbi.nlm.nih.gov/pmc/articles/PMC3316878). PMID 22395621 (https://pubmed.ncbi.nlm.nih.gov/22395621).
58. "Highest resolution microscope" (https://www.guinnessworldrecords.com/world-records/highest-resolution-microscope). *Guinness World Records*. Retrieved 18 July 2021.

59. Chen, Zhen; Jiang, Yi; Shao, Yu-Tsun; Holtz, Megan E.; Odstrčil, Michal; Guizar-Sicairos, Manuel; Hanke, Isabelle; Ganschow, Steffen; Schlom, Darrell G.; Muller, David A. (21 May 2021). "Electron ptychography achieves atomic-resolution limits set by lattice vibrations" (https://www.science.org/doi/10.1126/science.abg2533). *Science*. **372** (6544): 826–831. arXiv:2101.00465 (https://arxiv.org/abs/2101.00465). doi:10.1126/science.abg2533 (https://doi.org/10.1126%2Fscience.abg2533). ISSN 0036-8075 (https://www.worldcat.org/issn/0036-8075). PMID 34016774 (https://pubmed.ncbi.nlm.nih.gov/34016774). S2CID 230435950 (https://api.semanticscholar.org/CorpusID:230435950).
60. Blaustein, Anna. "See the Highest-Resolution Atomic Image Ever Captured" (https://www.scientificamerican.com/article/see-the-highest-resolution-atomic-image-ever-captured/). *Scientific American*. Retrieved 18 July 2021.
61. "Atomic Dodgeball" (https://www.scientificamerican.com/index.cfm/_api/render/file/?method=inline&fileID=2E4CCFB6-8C40-4213-AC2868D1C863EEB5). *Scientific American*. p. 16. Retrieved 27 August 2021.

External links

- Cornell researchers see atoms at record resolution (https://news.cornell.edu/stories/2021/05/cornell-researchers-see-atoms-record-resolution), cornell.edu at May 20, 2021
